Scaling Hidden Markov Language Models

Anonymous EMNLP submission

Abstract

The hidden Markov model (HMM) is a fundamental tool for sequence modeling that cleanly separates the hidden state from the emission structure. However, this clean separation makes it difficult to fit HMMs to large datasets in modern NLP, and they have fallen out of use due to very poor performance compared to fully observed models. This work revisits the challenge of scaling HMMs to language modeling datasets, taking ideas from recent approaches to neural modeling. We propose methods for scaling HMMs to massive state spaces while maintaining compact parameterization, effective regularization, and efficient exact inference. Experiments show that this approach leads to models that are much more accurate than previous HMMs and n-gram-based methods, making progress towards the performance of state-of-the-art NN models.

1 Introduction

Hidden Markov models (HMMs) are a fundamental latent-variable model for sequential data. Historically they have been used extensively in NLP for tasks such as sequence modeling (Rabiner, 1990), alignment (Vogel et al., 1996), and even, in a few cases, to language modeling (Kuhn et al., 1994; Huang, 2011). Compared to other approaches for sequence models, HMMs are naturally appealing since they fully separate out the process of sequential memory from the process of generation, while allowing for exact posterior inference.

State-of-the-art systems in NLP have moved away from utilizing latent hidden states and toward deterministic deep neural models. We take several lessons from the success of neural models for NLP tasks: (a) model size is critical for finding better local optima, e.g. large LSTMs (Zaremba et al., 2014) show marked improvements in performance;

(b) the right factorization is critically important for representation learning, e.g. a feedforward model (Bengio et al., 2003) can have the same probabilistic structure as an n-gram model while performing significantly better; (c) dropout is key to achieving strong performance on smaller datasets (Zaremba et al., 2014; Merity et al., 2017).

We revisit HMMs for language modeling, positing that competitive performance may require very large models. We make the following contributions: 1) We introduce a modeling constraint that allows us to utilize HMMs with large state spaces while maintaining efficient exact inference. 2) We develop a neural parameterization that improves generalization while remaining faithful to the probabilistic structure of the HMM. 3) Finally, we create a variant of dropout that both improves accuracy and reduces the computational overhead by an order of magnitude during training.

Experiments employ HMMs on two language modeling datasets, where we study the effect of scaling the state space of HMMs. Our three contributions allow us to train an HMM with tens of thousands of states, significantly outperforming past HMMs as well as n-gram models.

2 Related Work

In order to improve the performance of HMMs on language modeling, several recent papers have combined HMMs with neural networks. Buys et al. (2018) develop an approach to relax HMMs, but their models either perform poorly or alter the probabilistic structure to resemble an RNN. Krakovna and Doshi-Velez (2016) utilize model combination with an RNN to connect both approaches in a 20 state model. We demonstrate how to scale to orders of magnitude more states and show stronger performance.

Prior work has considered neural parameterizations of HMMs. Tran et al. (2016) demonstrate improvements in POS induction with a neural parameterization of an HMM. They consider small state spaces, as the goal was tag induction rather than language modeling. [1]

Prior work has also used HMMs with many states. Dedieu et al. (2019) introduce a sparsity constraint in order to train a 30K state HMM for character-level language modeling; however, their constraint precludes application to large vocabularies. We overcome this limitation and train models on word-level language modeling.

Finally, another approach to scaling to large state spaces is to grow from small to big via a split-merge process (Petrov et al., 2006; Huang, 2011). In particular, Huang (2011) learn an HMM for language modeling via this process. As fixed-size state spaces are significantly easier to optimize for GPUs, we leave split-merge procedures for future work.

3 Background: HMMs

We are interested in learning a distribution over observed tokens $\mathbf{x} = \langle x_1, \ldots, x_T \rangle$, with each token x_t an element of the finite vocabulary $\mathcal{X}$. Hidden Markov models (HMMs) specify a joint distribution over observed tokens $\mathbf{x}$ and discrete latent states $\mathbf{z} = \langle z_1, \ldots, z_T \rangle$, with each z_t from finite set $\mathcal{Z}$. For notational convenience, we define the starting state $z_0 = \epsilon$. This yields the joint distribution

$$p(\mathbf{x}, \mathbf{z}; \theta) = \prod_{t=1}^{T} p(x_t \mid z_t) p(z_t \mid z_{t-1}) \quad (1)$$

The distributions are parameterized as follows

$$p(z_t \mid z_{t-1}) \propto e^{\psi_{z_t z_{t-1}}} \quad p(x_t \mid z_t) \propto e^{\phi_{x_t z_t}} \quad (2)$$

with transitions $\psi \in \mathbb{R}^{|\mathcal{Z}| \times |\mathcal{Z}|}$ and emissions $\phi \in \mathbb{R}^{|\mathcal{X}| \times |\mathcal{Z}|}$. We refer to emissions $p(x_t \mid z_t)$ as $\mathbf{O}$.

We distinguish two types of parameterizations: *scalar* and *neural*. A scalar parameterization simply uses $\theta = \{\phi, \psi\}$ to fit one model parameter for each distributional parameter ($O(|\mathcal{Z}|^2 + |\mathcal{X}||\mathcal{Z}|)$ model parameters). A neural parameterization uses θ as parameters of a neural network that generates ϕ and ψ, which allows for factorization.

---

[1] Other work has used neural parameterization for structured models, such as dependency models (Han et al., 2017), hidden semi-Markov models (Wiseman et al., 2018), and context free grammars (Kim et al., 2019).
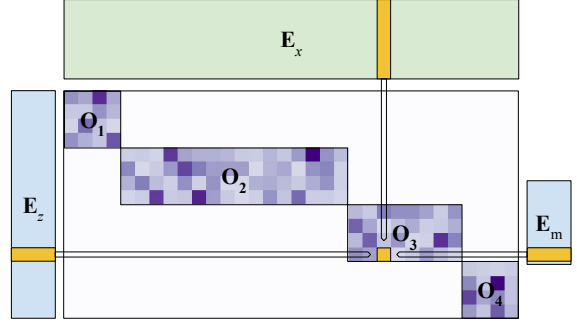

Figure 1: The emission matrix as a set of blocks $\mathbf{O}_1, \ldots, \mathbf{O}_4$ (shown in transpose). Each active cell is constructed from word, state, and block embeddings.

In order to fit an HMM to data $\mathbf{x}$, we must marginalize over the latent states to obtain the likelihood $p(\mathbf{x}) = \sum_{\mathbf{z}} p(\mathbf{x}, \mathbf{z})$. This sum can be computed in time $O(T|\mathcal{Z}|^2)$ via dynamic programming, which becomes prohibitive if the number of latent states $|\mathcal{Z}|$ is large. We can then optimize the likelihood with gradient ascent (or alternative variants of expectation maximization).

HMMs and RNNs Recurrent neural networks (RNNs) do not attempt to decouple the latent dynamics from the observed. This often leads to improved accuracy, but does not allow for posterior inference or for directly incorporating additional state information. These are inherently interesting properties worth exploring. A further benefit of HMMs over RNNs is that their associative structure allows for parallel inference via the prefix-sum algorithm (Ladner and Fischer, 1980). [2]

4 Scaling HMMs

Blocked Emissions Efficiency of marginal inference inherently limits the state space of general HMMs. However, we can improve inference complexity in special cases. As states in an HMM are used to represent context, a reasonable assumption is that not every word should be used in every context. Inspired by cloned HMMs (Dedieu et al., 2019), we constrain our HMMs to have rectangular fixed-width blocked emissions,

$$\mathbf{O} = \begin{bmatrix} \mathbf{O}^1 & 0 & 0 \\ 0 & \ldots & 0 \\ 0 & 0 & \mathbf{O}^M \end{bmatrix}$$

---

[2] Quasi-RNNs (Bradbury et al., 2016) also have a logarithmic dependency on T by applying the same prefix-sum trick, but do not model uncertainty over latent dynamics.
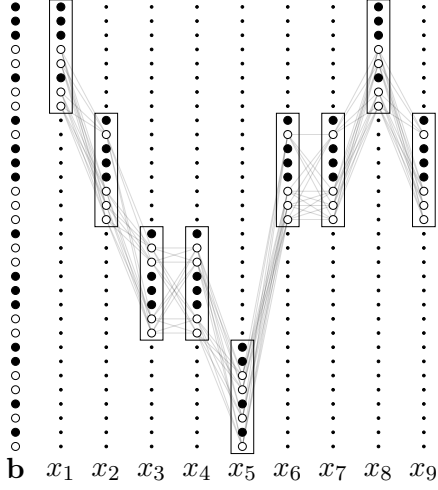
Figure 2: Computation of $p(\mathbf{x})$ is greatly reduced by blocked emissions and state dropout. Edges between nodes in the trellis indicate nonzero transition probabilities after clamping $\mathbf{x}$.

where each $\mathbf{O}_m \in \mathbb{R}^{\mathcal{X}_m \times |\mathcal{Z}|/M}$ is a partition indicating which tokens $\mathcal{X}_m$ can be emit by states $m|\mathcal{Z}|$ through $(m+1)|\mathcal{Z}|$. Conversely let $\mathcal{Z}_x \subset \mathcal{Z}$ be the states with non-zero probability of emitting x. Exact marginalization can be computed via

$$
\begin{aligned}
p(\mathbf{x}) = \sum_{z_1 \in \mathcal{Z}_{x_1}} p(z_1 \mid z_0) p(x_1 \mid z_1) \times \\
\cdots \sum_{z_T \in \mathcal{Z}_{x_T}} p(z_T \mid z_{T-1}) p(x_T \mid z_T)
\end{aligned}
\tag{3}
$$

This gives a serial complexity of $O(T(|\mathcal{Z}|/M)^2)$.

Factored Neural Parameterization Even with blocked emissions, the scalar parameterization of an HMM grows as $O(|\mathcal{Z}|^2)$. We instead employ a neural parameterization. The approach is to embed each state in $\mathcal{Z}$ ($\mathbf{E}_z \in \mathbb{R}^{|\mathcal{Z}| \times h/2}$), each token in $\mathcal{X}$ ($\mathbf{E}_x \in \mathbb{R}^{|\mathcal{X}| \times h}$), and each block ($\mathbf{E}_m \in \mathbb{R}^{M \times h/2}$). From these we can create representations for leaving and entering a state, and emitting a word:

$$
\mathbf{H}_{\text{out}}, \mathbf{H}_{\text{in}}, \mathbf{H}_{\text{emit}} = \text{MLP}(\mathbf{E}_m, \mathbf{E}_z)
$$

The HMM distributional parameters are given by,

$$
\phi = \mathbf{E}_x \mathbf{H}_{\text{emit}}^\top \quad \psi = \mathbf{H}_{\text{out}} \mathbf{H}_{\text{in}}^\top
\tag{4}
$$

where $\phi \in \mathbb{R}^{|\mathcal{X}| \times |\mathcal{Z}|}$ and $\psi \in \mathbb{R}^{|\mathcal{Z}| \times |\mathcal{Z}|}$. The MLP architecture follows (Kim et al., 2019), with details in the appendix. This neural parameterization takes $O(h^2 + h|\mathcal{Z}| + h|\mathcal{X}|)$ parameters (shown in Figure 1).

Algorithm 1 HMM Training

Given: block structure and model parameters
Sample block-wise dropout mask $\mathbf{b}$
Compute ϕ, ψ ignoring $b_z = 0$
for all batch examples $\mathbf{x}$ **do**
  $\Phi = \text{LOGPOTENTIALS}(\phi, \psi, \mathbf{x}, \mathbf{b})$
  $\log p(\mathbf{x}) = \text{FORWARD}(\Phi)$
Update embeddings $\mathbf{E}_{\mathbf{z}}, \mathbf{E}_{\mathbf{x}}, \mathbf{E}_\pi$

Note that parameter computation is independent of inference and can be cached completely at test-time. For training, we compute them once per batch (shown in Alg 1). For RNNs and similar models, emissions must be recomputed for each token.

Dropout as State Reduction To encourage full use of the state space, we introduce dropout that prevents the model from favoring specific states. We propose a form of HMM state dropout that removes states from use entirely, which has the added benefit of speeding up inference.

State dropout acts on each emission block $\mathbf{O}_1, \ldots, \mathbf{O}_M$ independently. For each block (with $|\mathcal{Z}|/M$ columns), we sample a binary dropout mask by sampling $\lambda \times (|\mathcal{Z}|/M)$ dropped row indices uniformly without replacement, where λ is the dropout rate. We concatenate these to a global vector $\mathbf{b}$, which, along with the previous constraints, ensures,

$$
p(x \mid z) \propto b_z 1(z \in \mathcal{Z}_x) e^{\phi_{xz}}
\tag{5}
$$

State dropout gives a large practical speed up for both parameter computation and inference. For $\lambda = 0.5$ we get a $4\times$ speed improvement for both, due to reduction of possible transitions. This structured dropout is also easier to exploit on GPU, since it maintains block structure with fixed-height (as shown in Figure 2).

5 Experimental Setup

Emission Blocks The model requires partitioning token types into blocks $\mathcal{X}_m$. While there are many partitioning methods, a natural choice is Brown clusters (Brown et al., 1992; Liang, 2005) which are also based on HMMs. Brown clusters are obtained by assigning every token type in $\mathcal{X}$ a state in an HMM, then merging states until a desired number of partitions M is reached. We construct the Brown clusters on the training portions of the datasets.

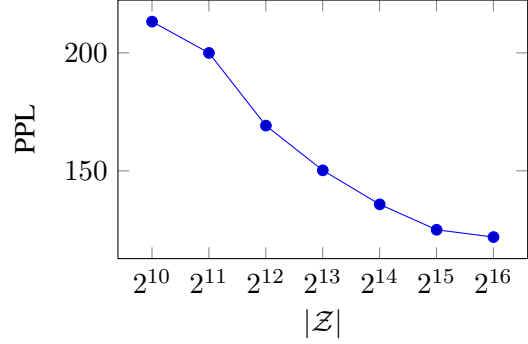| Model	Size	Val	Test
Penn Treebank			
KN 5-gram	2M	-	141.2
AWD-LSTM	24M	60.0	57.3
256 FF 5-gram	2.9M	159.9	152.0
2x256 dim LSTM	3.6M	93.6	88.8
HMM+RNN	10M	142.3	-
HMM ($|\mathcal{Z}|$=900)	10M	284.6	-
VL-NHMM ($|\mathcal{Z}| = 2^{15}$)	7.7M	125.0	115.8
WikiText			
KN 5-gram	5.7M	248.7	234.3
AWD-LSTM	33M	68.6	65.8
256 FF 5-gram	8.8M	210.9	195.0
2x256 LSTM	9.6M	124.5	117.5
VL-NHMM ($|\mathcal{Z}| = 2^{15}$)	13.7M	169.0	158.2

Table 1: Perplexities on the PTB / Wikitext-2.

Datasets We evaluate on the Penn Treebank (Marcus et al., 1993) (929k train tokens, 10k vocab) and wikitext2 (Merity et al., 2016) (2M train tokens, 33k vocab) datasets. For Penn Treebank we use the preprocessing from Mikolov et al. (2011), which lowercases all words and substitutes OOV words with unks. For Wikitext2 casing is preserved, and all OOV words are unked.

Baselines Baselines include AWD-LSTM (Merity et al., 2017); a 900-state scalar HMM and HMM+RNN extension, which discards the latent variable formulation (Buys et al., 2018); a KN 5-gram model (Mikolov and Zweig, 2012; Heafield et al., 2013), a 256 dimension FF model, and a 2-layer 256 dimension LSTM. We compare these models with our very large neural HMM (VL-NHMM, $|\mathcal{Z}| = 2^{15}$) that considers 256 latent states at every timestep at test time. [3] See the appendix for all hyperparameters.

6 Results

Table 1 gives the main results. On PTB, the VL-NHMM is able achieve 115.8 perplexity on the test set, outperforming a FF baseline and vastly outperforming the 900-state HMM from Buys et al. (2018). The VL-NHMM also outperforms the HMM+RNN extension of Buys et al.

---

[3] The 256 dim FF and LSTM models have comparable computational complexity to the VL-NHMM, taking computation $O(256^2 T)$.

Figure 3: Perplexity on PTB by state size $|\mathcal{Z}|$ ($\lambda = 0.5$ and $M = 128$).

Model	Size	Train	Val	Time
VL-NHMM (2^{14})	5.6M	122	136	48
- dropout	5.6M	89	145	100
- block emb	7.2M	115	134	40
- neural param	423M	119	169	14

Table 2: Ablations on PTB ($\lambda = 0.5$ and $M = 128$). Time is ms per eval batch (Run on RTX 2080).

(2018). [4] These results indicate that HMMs are a much stronger model on this benchmark than previously claimed. However, the VL-NHMM is outperformed by LSTMs. This trend persists in Wikitext-2, with the HMM outperforming the FF model but underperforming an LSTM.

Fig. 3 examines the effect of state size. We find that performance continuously improving significantly as we grow to 2^{16} states. Table 2 considers other ablations. We find that state dropout results in both an improvement in perplexity and a large improvement in time per epoch. Although neural and scalar parameterizations reach similar training perplexity, the neural model generalizes better on validation with almost 100x fewer parameters.

7 Conclusion

This work demonstrates that scaling HMMs to large states spaces results in gains in performance. We introduced three contributions: a blocked emission constraint, a neural parameterization, and state dropout. These contributions lead to an HMM that outperforms n-gram models and prior HMMs. This work demonstrates the classical probabilistic models can scale on modern hardware and are interesting option for fitting NLP datasets.

---

[4] Buys et al. (2018) only report validation perplexity.

References

Yoshua Bengio, Réjean Ducharme, Pascal Vincent, and Christian Janvin. 2003. A neural probabilistic language model. *J. Mach. Learn. Res.*, 3(null):1137–1155.

James Bradbury, Stephen Merity, Caiming Xiong, and Richard Socher. 2016. Quasi-recurrent neural networks. *CoRR*, abs/1611.01576.

Peter F. Brown, Peter V. deSouza, Robert L. Mercer, Vincent J. Della Pietra, and Jenifer C. Lai. 1992. Class-based n-gram models of natural language. *Comput. Linguist.*, 18(4):467–479.

Jan Buys, Yonatan Bisk, and Yejin Choi. 2018. Bridging hmms and rnns through architectural transformations.

Antoine Dedieu, Nishad Gothoskar, Scott Swingle, Wolfgang Lehrach, Miguel Lázaro-Gredilla, and Dileep George. 2019. Learning higher-order sequential structure with cloned hmms.

Wenjuan Han, Yong Jiang, and Kewei Tu. 2017. Dependency grammar induction with neural lexicalization and big training data. In *Proceedings of the 2017 Conference on Empirical Methods in Natural Language Processing*, pages 1683–1688, Copenhagen, Denmark. Association for Computational Linguistics.

Kenneth Heafield, Ivan Pouzyrevsky, Jonathan H. Clark, and Philipp Koehn. 2013. Scalable modified Kneser-Ney language model estimation. In *Proceedings of the 51st Annual Meeting of the Association for Computational Linguistics (Volume 2: Short Papers)*, pages 690–696, Sofia, Bulgaria. Association for Computational Linguistics.

Zhongqiang Huang. 2011. *Modeling Dependencies in Natural Languages with Latent Variables*. Ph.D. thesis, University of Maryland.

Yoon Kim, Chris Dyer, and Alexander M. Rush. 2019. Compound probabilistic context-free grammars for grammar induction. *CoRR*, abs/1906.10225.

Viktoriya Krakovna and Finale Doshi-Velez. 2016. Increasing the interpretability of recurrent neural networks using hidden markov models.

Thomas Kuhn, Heinrich Niemann, and Ernst Günter Schukat-Talamazzini. 1994. Ergodic hidden markov models and polygrams for language modeling. pages 357–360.

Richard E. Ladner and Michael J. Fischer. 1980. Parallel prefix computation. *J. ACM*, 27(4):831–838.

Percy Liang. 2005. Semi-supervised learning for natural language. In *MASTER'S THESIS, MIT*.

Ilya Loshchilov and Frank Hutter. 2017. Fixing weight decay regularization in adam. *CoRR*, abs/1711.05101.

Mitchell P. Marcus, Beatrice Santorini, and Mary Ann Marcinkiewicz. 1993. Building a large annotated corpus of English: The Penn Treebank. *Computational Linguistics*, 19(2):313–330.

Stephen Merity, Nitish Shirish Keskar, and Richard Socher. 2017. Regularizing and optimizing LSTM language models. *CoRR*, abs/1708.02182.

Stephen Merity, Caiming Xiong, James Bradbury, and Richard Socher. 2016. Pointer sentinel mixture models. *CoRR*, abs/1609.07843.

T. Mikolov and G. Zweig. 2012. Context dependent recurrent neural network language model. In *2012 IEEE Spoken Language Technology Workshop (SLT)*, pages 234–239.

Tomas Mikolov, Anoop Deoras, Stefan Kombrink, Lukás Burget, and Jan Cernocký. 2011. Empirical evaluation and combination of advanced language modeling techniques. pages 605–608.

Slav Petrov, Leon Barrett, Romain Thibaux, and Dan Klein. 2006. Learning accurate, compact, and interpretable tree annotation. page 433–440.

Lawrence R. Rabiner. 1990. *A Tutorial on Hidden Markov Models and Selected Applications in Speech Recognition*, page 267–296. Morgan Kaufmann Publishers Inc., San Francisco, CA, USA.

Ke M. Tran, Yonatan Bisk, Ashish Vaswani, Daniel Marcu, and Kevin Knight. 2016. Unsupervised neural hidden markov models. *CoRR*, abs/1609.09007.

Stephan Vogel, Hermann Ney, and Christoph Tillmann. 1996. Hmm-based word alignment in statistical translation. In *Proceedings of the 16th Conference on Computational Linguistics - Volume 2*, COLING '96, page 836–841, USA. Association for Computational Linguistics.

Sam Wiseman, Stuart M. Shieber, and Alexander M. Rush. 2018. Learning neural templates for text generation. *CoRR*, abs/1808.10122.

Wojciech Zaremba, Ilya Sutskever, and Oriol Vinyals. 2014. Recurrent neural network regularization. *CoRR*, abs/1409.2329.

A Appendices

A.1 Hyperparameters

For `Penn Treebank` and `Wikitext-2`, we trained the following baselines: a two layer feedforward 5-gram model and a two layer LSTM. The feedforward model is given by the following:

$$p(w_t \mid \mathbf{w}_{<t}) = W_x \text{ReLU}(\text{Conv}(\mathbf{E}_w(\mathbf{w}_{t-4:t-1}))) \quad (6)$$

where $\mathbf{E}_w$ gives the word embeddings and $W_x \in \mathbb{R}^{|\mathcal{X}| \times h}$ is weight-tied to the embeddings.

For the feedforward model we use a batch size of 128 and a bptt length of 64, as we found the model needed a larger batch size to train. For the LSTM, we use a batch size of 16 and a BPTT length of 32. For both baseline models we use AdamW (Loshchilov and Hutter, 2017) with a learning rate of 1e-3 and a dropout rate of 0.3 on the activations in the model. Both models use a hidden dimension of 256 throughout. These same hyperparameters were applied on both `Penn Treebank` and `Wikitext-2`.

For the HMMs we use a batch size of 16 and a BPTT length of 32. We use state dropout with $\lambda = 0.5$. We use AdamW (Loshchilov and Hutter, 2017) with a learning rate of 1e-2 for `Penn Treebank`, and a learning rate of 1e-3 for `Wikitext-2`.

All weights are initialized with the Kaiming uniform initialization.

Hyperparameter search was performed manually, using validation perplexity.

A.2 HMM Parameterization

Let $\mathbf{E}, \mathbf{D} \in \mathbb{R}^{v \times h}$ be an embedding matrix and a matrix of the same size, where v is the size of the vocab and h the hidden dimension. We use the following residual network:

$$f_i(\mathbf{E}) = g_i(\text{ReLU}(\mathbf{E}W_{i1}))$$
$$g_i(\mathbf{D}) = \text{LayerNorm}(\text{ReLU}(\mathbf{D}W_{i2}) + \mathbf{D}) \quad (7)$$

with $i \in \{\text{out}, \text{in}, \text{emit}\}$, $W_{i1}, W_{i2} \in \mathbb{R}^{h \times h}$ where h is the hidden dimension.

For the factored state embeddings in Sec. 4, we introduce residual networks $f_j, j \in \{o, i, e\}$ to compose block and state embeddings, yielding

$$\mathbf{H}_{\text{out}} = f_{\text{out}}(f_o([\mathbf{E}_m, \mathbf{E}_z]))$$
$$\mathbf{H}_{\text{in}} = f_{\text{in}}(f_i([\mathbf{E}_m, \mathbf{E}_z])) \quad (8)$$
$$\mathbf{H}_{\text{emit}} = f_{\text{emit}}(f_e([\mathbf{E}_m, \mathbf{E}_z]))$$

Constraint	$|\mathcal{Z}|$	$|\mathcal{C}_x|$	m	Val PPL
Brown	16384	512	32	137
Brown	16384	256	64	138
Brown	16384	128	128	134
Brown	16384	64	256	136
None	1024	-	-	180
Brown	1024	256	4	182
Brown	1024	128	8	194
Uniform	8192	128	-	150
Brown	8192	128	64	142
Uniform	16384	128	-	146
Brown	16384	128	128	136

Table 3: Emission constraint ablations on `Penn Treebank`.

A.3 Emission constraint ablation

Tbl. 3 shows the results from emission constraint ablations. For the ablations in this section, we do not use the factored state embedding and instead directly learn embeddings $\mathbf{E}_z \in \mathbb{R}^{|\mathcal{Z}| \times h}$. We examine the effect of factored state embeddings in the next section.

With a VL-NHMM that has $|\mathcal{Z}| = 2^{14}$ states, the model is insensitive to the number of blocks M. However, with fewer states $|\mathcal{Z}| = 2^{10}$ where we are able to able to use fewer blocks to examine whether the block-sparsity of the emission results in a performance loss. With $M = 4$ blocks, the block-sparse HMM matches an unconstrained HMM with the same number of states. When $M = 8$, the block-sparse model underperforms, implying there may be room for improvement with the larger HMMs that use $M > 8$ blocks.

We additionally compare the blocks induced by Brown clustering with a uniform constraint that samples subsets of states of size n independently and uniformly from $\mathcal{Z}$. This does not admit a partitioning, which makes it difficult to apply state dropout. We therefore zero out half of the logits of the transition matrix randomly before normalization. In the bottom of Tbl. 3, we find that models with uniform constraints are consistently outperformed by models with Brown cluster constraints as measured by validation perplexity. The models with uniform constraints also had poor validation performance despite better training performance, a symptom of overfitting.

These ablations demonstrate that the constraints

6

based on Brown clusters used in this work may not be optimal, motivating future work that learns sparsity structure.

A.4 Factored state embedding ablation

The results of the factored state ablation are in Fig. 4. We find that the performance of independent state embeddings with is similar to a model with factored embeddings, until the number of blocks is ≤ 64.
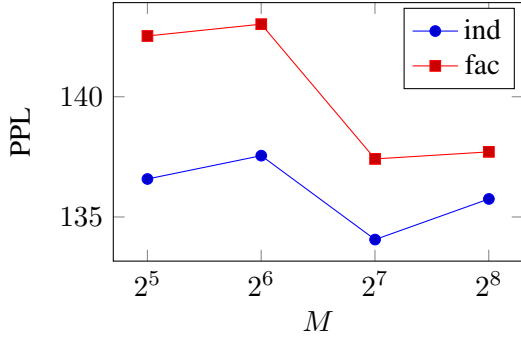

Figure 4: Perplexity on PTB by state size $|\mathcal{Z}|$ ($\lambda = 0.5$ and $M = 128$).